

Received 10 March 2019
Accepted 26 June 2019

Edited by Y. Ohgo, Teikyo University, Japan

Keywords: macozinone; crystal structure; synthesis; drug sensitive; drug resistant; tuberculosis.

CCDC reference: 1572644

Supporting information: this article has supporting information at journals.iucr.org/c

Macozinone: revised synthesis and crystal structure of a promising new drug for treating drug-sensitive and drug-resistant tuberculosis

Gang Zhang^{a*} and Courtney C. Aldrich^{a,b*}

^aState Key Laboratory of Bioactive Substances and Function of Natural Medicine, Institute of Materia Medica, Peking Union Medical College and Chinese Academy of Medical Sciences, Beijing 100050, People's Republic of China, and

^bDepartment of Medicinal Chemistry, University of Minnesota, Minneapolis, Minnesota 55455, USA. *Correspondence e-mail: gzhang@imm.ac.cn, aldri015@umn.edu

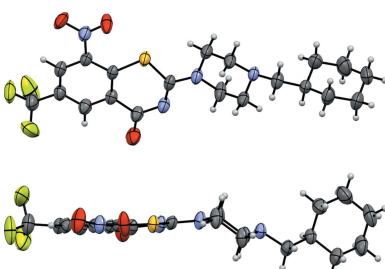
Mycobacterium tuberculosis (*Mtb*), the principal etiological agent of tuberculosis (TB), infects over one-quarter of humanity and is now the leading cause of infectious disease mortality by a single pathogen. Macozinone {2-[4-(cyclohexylmethyl)piperazin-1-yl]-8-nitro-6-(trifluoromethyl)-4H-1,3-benzothiazin-4-one, $C_{20}H_{23}F_3N_4O_3S$ } is a promising new drug for treating drug-sensitive and drug-resistant TB that has successfully completed phase I clinical trials. We report the complete spectroscopic and structural characterization by 1H NMR, ^{13}C NMR, HRMS, IR, and X-ray crystallography. The cyclohexyl moiety is observed to be nearly perpendicular to the core formed by the 1,3-benzothiazin-4-one and piperazine groups. The central piperazine ring adopts a slightly distorted chair conformation caused by sp^2 -hybridization of the nitro N atom, which donates into the electron-deficient 1,3-benzothiazin-4-one group.

1. Introduction

Tuberculosis (TB) caused by *Mycobacterium tuberculosis* (*Mtb*) is the leading source of infectious disease mortality by a single pathogen (WHO, 2018). The emergence of drug-resistant (DR) TB, HIV co-infection, and comorbidity with type II diabetes mellitus further complicates treatment options and demands a new generation of TB drugs effective against DR-TB, compatible with HIV antiretrovirals, and strongly bactericidal to overcome the impaired host immune system in diabetic and HIV patients.

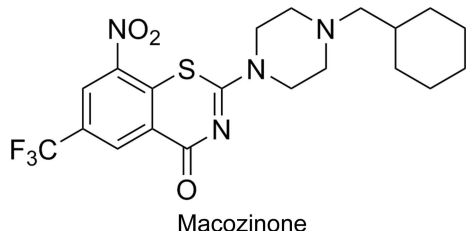
1,3-Benzothiazin-4-ones (BTZs) are a novel class of TB drug candidates that possess potent activity against both drug-susceptible and drug-resistant *Mtb* strains (Makarov *et al.*, 2009). Biochemical and genetic studies revealed that BTZs inhibit decaprenylphosphoryl- β -D-ribose 2'-epimerase (DprE1, Rv3790), which is a critical flavoenzyme involved in the biosynthesis of the mycobacterial cell wall (Makarov *et al.*, 2009). BTZs are bioactivated by the dihydroflavin cofactor FADH₂ of DprE1 through reduction of the C-8 nitro group to a nitroso intermediate, which covalently reacts with Cys387 in the enzyme active site to form a semi-mercaptal enzyme-inhibitor adduct (Trefzer *et al.*, 2010). Macozinone (PBTZ169) is the most potent BTZ derivative yet described with subnanomolar whole-cell activity and has successfully completed phase I clinical trials. The extraordinary potency of macozinone is derived from its covalent mode of inhibition, as well as the cellular location of the target DprE1 (Trefzer *et al.*, 2010, 2012; Neres *et al.*, 2012; Brecik *et al.*, 2015).

Herein we report the synthesis of macozinone using the classic Makarov route to the BTZs (Makarov *et al.*, 2007), but



© 2019 International Union of Crystallography

with slight modification to prepare the requisite 2-chloro-3-nitro-5-(trifluoromethyl)benzamide building block that avoids generation of the reactive acid chloride. Macozinone (see Scheme) was fully characterized by single-crystal X-ray diffraction (XRD) analysis.



2. Experimental

2.1. Chemical synthesis

All chemicals were obtained from commercial sources and used without further preparation. 2-Chloro-3-nitro-5-(trifluoromethyl)benzoic acid was prepared as described (Makarov *et al.*, 2014). Proton and carbon NMR spectra were recorded in deuterated solvents on a Varian Mercury 400 MHz spectrometer. The chemical shifts are reported in parts per million (δ) relative to an internal tetramethylsilane (TMS) standard. Coupling constants are reported in Hertz. IR spectra were recorded on a Bruker TENSOR FT-IR spectrometer. Melting points were determined using a Yanaco melting-point apparatus and are uncorrected. Mass spectra were determined on an Exactive Plus LC/MSD Orbitrap from Thermo Fisher Scientific.

2.1.1. 2-Chloro-3-nitro-5-(trifluoromethyl)benzamide (2). To a stirred solution of 2-chloro-3-nitro-5-(trifluoromethyl)benzoic acid (2.7 g, 10 mmol, 1.0 equiv.), pyridine (0.50 ml, 6.2 mmol, 0.62 equiv.), and Boc₂O (2.8 g, 13.0 mmol, 1.3 equiv.) in 1,4-dioxane (10 ml) at room temperature was added ammonium bicarbonate (1.00 g, 12.6 mmol, 1.26 equiv.). The reaction was stirred overnight at room temperature and then partitioned between EtOAc (50 ml) and H₂O (50 ml). The organic layer was separated, washed consecutively with water

Table 1
Experimental details.

Crystal data	
Chemical formula	C ₂₀ H ₂₃ F ₃ N ₄ O ₃ S
M _r	456.48
Crystal system, space group	Monoclinic, P2 ₁ /c
Temperature (K)	205
a, b, c (Å)	15.051 (7), 5.295 (2), 26.548 (11)
β (°)	97.372 (7)
V (Å ³)	2098.3 (15)
Z	4
Radiation type	Mo K α
μ (mm ⁻¹)	0.21
Crystal size (mm)	0.16 × 0.15 × 0.12
Data collection	
Diffractometer	Bruker D8 Venture
Absorption correction	Multi-scan (SADABS; Bruker, 2013)
T_{\min} , T_{\max}	0.641, 0.746
No. of measured, independent and observed [$I > 2\sigma(I)$] reflections	11854, 4794, 3412
R _{int}	0.025
(sin θ/λ) _{max} (Å ⁻¹)	0.654
Refinement	
$R[F^2 > 2\sigma(F^2)]$, wR(F^2), S	0.047, 0.122, 1.05
No. of reflections	4794
No. of parameters	326
No. of restraints	36
H-atom treatment	H-atom parameters constrained
$\Delta\rho_{\max}$, $\Delta\rho_{\min}$ (e Å ⁻³)	0.29, -0.21

Computer programs: APEX2 (Bruker, 2013), SAINT (Bruker, 2013), SHELXT (Sheldrick, 2015a), SHELXL2018 (Sheldrick, 2015b) and OLEX2 (Dolomanov *et al.*, 2009).

(50 ml) and 0.6 N aqueous HCl (50 ml), dried (Mg₂SO₄), and filtered. The filtrate was concentrated under reduced pressure to provide **2** as a white solid [yield 2.42 g, 90%; m.p. 190–193 °C; literature (Welch *et al.*, 1969) 195–197 °C]. ¹H NMR and MS data are consistent with previously reported spectra (Cooper *et al.*, 2013).

2.1.2. 2-[4-(Cyclohexylmethyl)piperazin-1-yl]-8-nitro-6-(trifluoromethyl)-4H-1,3-benzothiazin-4-one (macozinone). Potassium carbonate (0.62 g, 4.5 mmol, 1.2 equiv.) was added to a

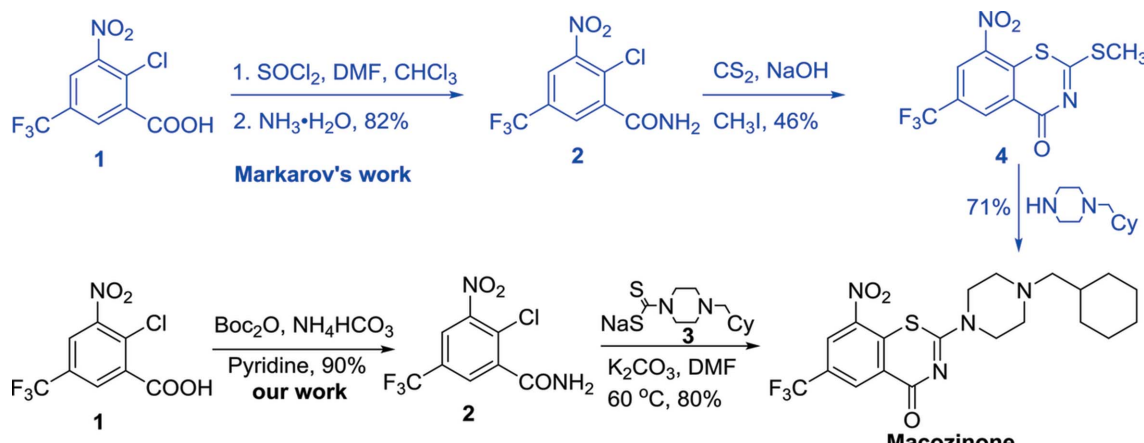


Figure 1

The synthesis of macozinone beginning from 2-chloro-3-nitro-5-(trifluoromethyl)benzoic acid (**1**), which was directly converted to the benzamide derivative (**2**). Condensation of **2** with sodium 4-(cyclohexylmethyl)piperazine-1-carbodithioate (**3**) afforded macozinone. The synthesis of macozinone reported by Makarov *et al.* (2014) is highlighted in blue.

solution of 2-chloro-3-nitro-5-(trifluoromethyl)benzamide (**2**; 1.0 g, 3.7 mmol, 1.0 equiv.), and sodium 4-(cyclohexylmethyl)piperazine-1-carbodithioate (**3**; 1.25 g, 4.5 mmol, 1.2 equiv.), in dimethylformamide (DMF, 20 ml). The mixture was heated at 60 °C for 2 h and then cooled to room temperature. The mixture was filtered and the filtrate was concentrated under reduced pressure. The crude product was purified by flash chromatography (petroleum ether/ethyl acetate 10:1 → 5:1 → 2:1 → 1:1 → 1:2 → 1:10 → 100% ethyl acetate) on silica gel to afford the title compound (yield 1.36 g, 80%) as a yellow solid [m.p. 185–187 °C; literature (Makarov *et al.*, 2014) 184–186 °C]; ^1H NMR (400 MHz, CDCl_3): δ 9.10 (*d*, $J = 2.1$ Hz, 1H), 8.75 (*d*, $J = 2.1$ Hz, 1H), 3.87–4.15 (*m*, 4H), 2.47–2.60 (*m*, 4H), 2.17–2.20 (*m*, 2H), 1.68–1.80 (*m*, 4H), 1.50–1.58 (*m*, 1H), 1.19–1.25 (*m*, 4H), 0.84–0.93 (*m*, 2H); ^{13}C NMR (100 MHz, CDCl_3): δ 166.5, 162.0, 143.9, 134.1, 133.4 (*q*, $^4J_{\text{C}-\text{F}} = 4.0$ Hz), 129.7 (*q*, $^2J_{\text{C}-\text{F}} = 35.0$ Hz), 126.8, 126.0 (*q*, $^3J_{\text{C}-\text{F}} = 4.0$ Hz), 122.4 (*q*, $^1J_{\text{C}-\text{F}} = 271$ Hz), 65.1, 53.1, 46.6, 35.0, 31.7, 26.7, 26.0; IR (KBr) ν (cm $^{-1}$) 2923, 1649, 1298, 1141, 1000, 916, 863, 781; HRMS (ESI-TOF $^+$) m/z [M + H] $^+$ calculated for $\text{C}_{20}\text{H}_{24}\text{F}_3\text{N}_4\text{O}_3\text{S}^+$ 457.1516; found 457.1521 (error 1.1 ppm).

2.2. Crystal growth of macozinone

Macozinone (5.0 mg) was suspended in ethyl acetate (EtOAc , 1 ml) and stirred vigorously at room temperature for 16 h. The remaining solid was removed by gravity filtration and the filtrate was transferred to a 5 ml glass tube. Hexane (3.0 ml) was added slowly on top of the saturated EtOAc solution of macozinone. The tube was capped and placed in a cool cabinet in the dark to promote crystallization. After 7 d, crystals suitable for X-ray diffraction analysis had formed.

2.3. Crystal data of macozinone

A search of the Cambridge Structural Database (CSD, Version 5.37; Groom *et al.*, 2016) and *Scifinder* (Version of 2018, <https://www.cas.org/products/scifinder>) revealed no hits. Crystal data, data collection and structure refinement details are summarized in Table 1. H atoms were placed in calculated positions and included as riding contributions with isotropic displacement parameters. H atoms belonging to aryl groups were located in difference density maps and were refined freely. The aryl H atoms were constrained with C–H = 0.95 Å, the methylene groups with C–H = 0.99 Å [$U_{\text{iso}}(\text{H}) = 1.2U_{\text{eq}}(\text{C})$] and the methyl groups with C–H = 0.98 Å [$U_{\text{iso}}(\text{H}) = 1.5U_{\text{eq}}(\text{C})$].

3. Results and discussion

3.1. Chemical synthesis

The synthesis of macozinone is shown in Fig. 1, beginning from 2-chloro-3-nitro-5-(trifluoromethyl)benzoic acid (Makarov *et al.*, 2014) (**1**), which was directly converted to the benzamide derivative (**2**) in 90% yield under mild room-temperature conditions by activation with di-*tert*-butyl dicarbonate (Boc_2O) and subsequent *in situ* reaction with ammonia derived from ammonium bicarbonate. Condensation of **2** with sodium

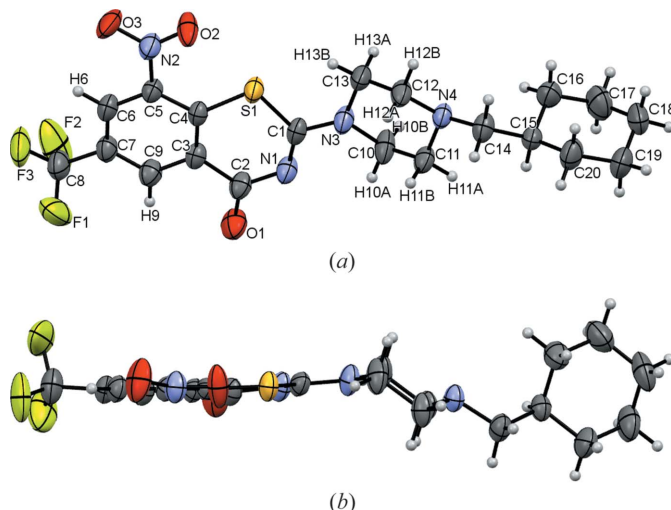


Figure 2
(a) The molecular structure of macozinone and (b) a structural side view of macozinone.

4-(cyclohexylmethyl)piperazine-1-carbodithioate (Makarov *et al.*, 2007) (**3**) in DMF using the conditions developed by Makarov *et al.* (2007) for the synthesis of earlier BTZ derivatives, through nucleophilic aromatic substitution followed by intramolecular cyclization and concomitant expulsion of hydrogen sulfide, afforded macozinone in 80% yield. Macozinone was fully characterized by ^1H NMR, ^{13}C NMR, HRMS and IR spectroscopy, and single-crystal X-ray diffraction analysis. Previously, only ^1H NMR and HRMS data has been provided for macozinone (Makarov *et al.*, 2014). For comparison, we have illustrated the synthesis of macozinone reported by Makarov (Fig. 1, highlighted in blue), which also began from **1**, but used refluxing conditions with thionyl chloride in CHCl_3 to obtain the acid chloride that was reacted with ice-cold ammonium hydroxide under Schotten–Baumann conditions to yield **2** (Cooper *et al.*, 2013). Reaction of **2** with carbonyl disulfide afforded 2-(methylsulfanyl)-8-nitro-6-(trifluoromethyl)-4*H*-thiochromen-4-one, **4**, which was subsequently condensed with 5-(cyclohexylmethyl)piperazine to afford macozinone in 71% yield (Makarov *et al.*, 2014).

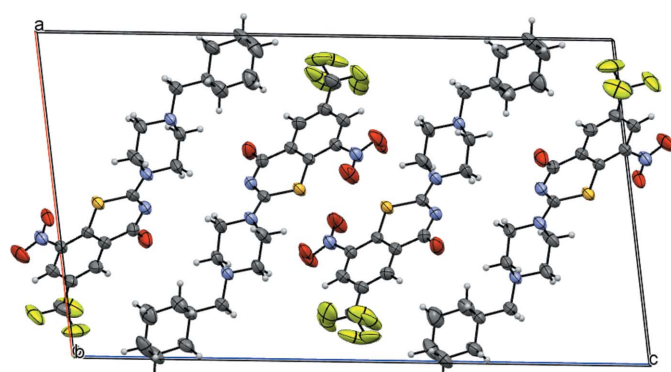


Figure 3
Outline of the unit cell with axes, showing all the molecular entities in the crystal. Partial crystal disorder exists at the nitro and trifluoromethyl positions of the target compound.

3.2. Crystal data

A search of the Cambridge Structural Database (CSD, Version 5.37; Groom *et al.*, 2016) for the thiopyran-4-one fragment resulted in 42 hits, of which 10 possessing the most similar structures were compared with those of the title compound (Table S5 in the supporting information) (Narasimhamurthy *et al.*, 2003; Duvvuru *et al.*, 2012; Gendron *et al.*, 2015; Rosiak *et al.*, 2006; Schmidt *et al.*, 2005; Ramalingam *et al.*, 1979; Xu *et al.*, 2015; Wang *et al.*, 2011; Mojtabahi *et al.*, 2011; Karisalmi *et al.*, 2003). This is the first small-molecule crystal structure reported for macozinone or any BTZ analogue.

Macozinone crystallized in the monoclinic system space group $P2_1/c$ (Fig. 2). The key feature of macozinone is the planar 1,3-benzothiazin-4-one heterocycle. The dihedral angle between 1,3-benzothiazin-4-one and the least-squares plane of the appended piperazine ring is $38.56(5)^\circ$. The cyclohexyl ring is almost perpendicular to the 1,3-benzothiazin-4-one and piperazine core. In the 1,3-benzothiazin-4-one fragment, the C1—S1 bond length is $1.776(2)$ Å, which is very close to the reported literature values (Narasimhamurthy *et al.*, 2003; Duvvuru *et al.*, 2012; Gendron *et al.*, 2015; Rosiak *et al.*, 2006; Schmidt *et al.*, 2005; Ramalingam *et al.*, 1979; Xu *et al.*, 2015; Wang *et al.*, 2011; Mojtabahi *et al.*, 2011; Karisalmi *et al.*, 2003). Similarly, the C4—S1 bond length of $1.739(2)$ Å and the C1—S1—C4 bond angle of $100.61(10)^\circ$ are comparable to the control crystal structures (Table S4 in the supporting information). Interestingly, the C1—N3 bond length of $1.330(2)$ Å is much shorter than the calculated C—N bond of *N*-methyl-piperazine (1.455 Å). The C1—N3—C13, C1—N3—C10, and C10—N3—C13 angles are $125.62(17)$, $120.85(19)$, and $113.11(17)^\circ$, respectively, which indicates that atom N3 is sp^2 -hybridized, driven by resonance stabilization of the nitrogen lone-pair into the electron-deficient 1,3-benzothiazin-4-one moiety. The piperazine ring in the structure adopts a slightly distorted chair conformation due to the sp^2 -hybridization of atom N3, with atoms N3 and N4 deviating by 0.689 and 0.591 Å, respectively, from the least-squares plane defined by atoms C10/C11/C12/C13.

In the crystal lattice of macozinone, there are four molecules in each cell unit (Fig. 3). Strong intermolecular hydrogen-bond interactions were observed between the O atoms of the NO_2 group and atoms H12B and H13B of the 1,4-piperazine moiety ($\text{N}2—\text{O}2\cdots\text{H}13B$ and $\text{N}2—\text{O}3\cdots\text{H}12B$;

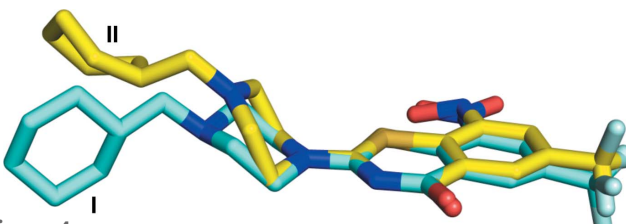


Figure 4
Overlay of small-molecule crystal of macozinone and its fragment from the cocrystal with DprE1 (PDB code: 4ncr). The small-molecule crystal structure of macozinone is shown as a cyan stick structure (denoted I) and the fragment of macozinone from the cocrystal with DprE1 is shown as a yellow stick structure (denoted II).

Table 2
Hydrogen-bond geometry (Å, °).

$D—\text{H}\cdots A$	$D—\text{H}$	$\text{H}\cdots A$	$D\cdots A$	$D—\text{H}\cdots A$
$\text{N}2—\text{O}2\cdots\text{H}12B$	$0.98(1)$	$2.68(1)$	$3.311(3)$	$123(1)$
$\text{N}2—\text{O}3\cdots\text{H}13B$	$0.98(1)$	$2.94(1)$	$3.844(15)$	$153(1)$

Table 2 and Fig. S2 in the supporting information), as well as the N1 atoms of the 1,3-benzothiazin-4-one group and atom H10A of 1,4-piperazine (C10—H10A···N1; Fig. S1 in the supporting information). The supermolecular aggregate was formed *via* the stronger intermolecular hydrogen bond in three dimensions, which promoted crystallization along the *bc*-axis direction in the crystal lattice and crystallization of macozinone in the space group $P2_1/c$.

The crystal structure of the reduced nitroso derivative of macozinone covalently bound to DprE1 (PDB code: 4ncr) was determined by Cole and co-workers (Makarov *et al.*, 2014). Comparison of our single-molecule crystal and the reduced nitroso macozinone structure of the complex with DprE1 revealed significant differences in the conformations of the piperazine and cyclohexyl rings. The small-molecule crystal structure (Fig. 4, I) displays a lower energy classic chair conformation for the cyclohexyl ring, but a twist-boat conformation is observed in the adduct structure (Fig. 4, II), which is presumably caused by the sterically congested environment in the enzyme active site. Similarly, the piperazine adopts the lowest-energy chair conformation in the single-molecule structure, but a higher-energy distorted chair conformation in the adduct structure. The implications of this work directly impinge on future drug-discovery efforts and suggest the introduction of conformational constraints onto the piperazine ring of macozinone that enforce the higher-energy twist-boat conformation (Fig. 4, II) may further enhance potency. Modifications of drugs that reduce molecular symmetry and planarity have been shown to improve aqueous solubility which can in turn enhance membrane permeability, oral bioavailability, and drug distribution in the body (Ishikawa *et al.*, 2011; Degorce *et al.*, 2018; Zhang *et al.*, 2019).

4. Conclusion

Macozinone is a promising new drug for treating drug-sensitive and drug-resistant TB that has successfully completed phase I clinical trials. We report the complete spectroscopic and structural characterization of macozinone by ^1H NMR, ^{13}C NMR, HRMS, IR, and X-ray crystallography. The cyclohexyl group is nearly perpendicular to the core formed by the 1,3-benzothiazin-4-one and piperazine groups. The central piperazine ring adopts a slightly distorted chair conformation caused by the sp^2 hybridization of the N2 atom, which donates into the electron-deficient 1,3-benzothiazin-4-one group.

Acknowledgements

We are grateful to the Center of Pharmaceutical Polymorphs, Institute of Materia Medica, Chinese Academy of Medical

Sciences, and Peking Union Medical College for providing instrument facilities. GZ thanks Dr Hualong Chen for assistance with the crystal data collection and processing.

Funding information

Funding for this research was provided by: the CAMS Innovation Fund for Medical Sciences (grant No. CAMS-2017-I2M-1-011).

References

- Brecik, M., Centárová, I., Mukherjee, R., Kolly, G. S., Huszár, S., Bobovská, A., Kilacsková, E., Mokošová, V., Svetlíková, Z., Šarkan, M., Neres, J., Korduláková, J., Cole, S. T. & Mikušová, K. (2015). *Chem. Biol.* **10**, 1631–1636.
- Bruker (2013). *APEX2, SAINT, and SADABS*. Bruker AXS Inc. Madison, Wisconsin, USA.
- Cooper, M. A., Zuegg, J., Becker, B. & Tomislav, K. (2013). Patent EP2570413.
- Degorce, S. L., Bodnarchuk, M. S., Cumming, I. A. & Scott, J. S. (2018). *J. Med. Chem.* **61**, 8934–8943.
- Dolomanov, O. V., Bourhis, L. J., Gildea, R. J., Howard, J. A. K. & Puschmann, H. (2009). *J. Appl. Cryst.* **42**, 339–341.
- Duvvuru, D., Pinto, N., Gomez, C., Betzer, J. F., Retailleau, P., Voituriez, A. & Marinetti, A. (2012). *Adv. Synth. Catal.* **354**, 408–414.
- Gendron, T., Kessedjian, H., Davioud-Charvet, E. & Lanfranchi, D. A. (2015). *Eur. J. Org. Chem.* **2015**, 1790–1796.
- Groom, C. R., Bruno, I. J., Lightfoot, M. P. & Ward, S. C. (2016). *Acta Cryst. B* **72**, 171–179.
- Ishikawa, M. & Hashimoto, Y. (2011). *J. Med. Chem.* **54**, 1539–1554.
- Karisalmi, K., Koskinen, A. M. P., Nissinen, M. & Rissanen, K. (2003). *Tetrahedron*, **59**, 1421–1427.
- Makarov, V. A., Cole, S. T. & Moellmann, U. (2007). WO Patent 2007134625 A1.
- Makarov, V., Lechartier, B., Zhang, M., Neres, J., van der Sar, A. M., Raadsen, S. A., Hartkoorn, R. C., Ryabova, O. B., Vocat, A., Decosterd, L. A., Widmer, N., Buclin, T., Bitter, W., Andries, K., Pojer, F., Dyson, P. J. & Cole, S. T. (2014). *EMBO Mol. Med.* **6**, 372–383.
- Makarov, V., et al. (2009). *Science*, **324**, 801–804.
- Mojtahedi, M., Abaee, M., Khakbaz, M., Alishiri, T., Samianifard, M., Mesbah, A. & Harms, K. (2011). *Synthesis*, **2011**, 3821–3826.
- Narasimhamurthy, T., Benny, J. C. N., Pandiarajan, K. & Rathore, R. S. (2003). *Acta Cryst. C* **59**, o620–o621.
- Neres, J., Pojer, F., Molteni, E., Chiarelli, L. R., Dhar, N., Boy-Rottger, S., Buroni, S., Fullam, E., Degiacomi, G., Lucarelli, A. P., Read, R. J., Zanoni, G., Edmondson, D. E., De Rossi, E., Pasca, M. R., McKinney, J. D., Dyson, P. J., Riccardi, G., Mattevi, A., Cole, S. T. & Binda, C. (2012). *Sci. Transl. Med.* **4**, 150ra121.
- Ramalingam, K., Berlin, K. D., Loghry, R. A., Van der Helm, D. & Satyamurthy, N. (1979). *J. Org. Chem.* **44**, 477–486.
- Rosiak, A., Frey, W. & Christoffers, J. (2006). *Eur. J. Org. Chem.* **2006**, 4044–4054.
- Schmidt, K., Kopf, J. & Margaretha, P. (2005). *Helv. Chim. Acta*, **88**, 1922–1930.
- Sheldrick, G. M. (2015a). *Acta Cryst. A* **71**, 3–8.
- Sheldrick, G. M. (2015b). *Acta Cryst. C* **71**, 3–8.
- Trefzer, C., Rengifo-Gonzalez, M., Hinner, M. J., Schneider, P., Makarov, V., Cole, S. T. & Johnsson, K. (2010). *J. Am. Chem. Soc.* **132**, 13663–13665.
- Trefzer, C., Škvorová, H., Buroni, S., Bobovská, A., Nenci, S., Molteni, E., Pojer, F., Pasca, M. R., Makarov, V., Cole, S. T., Riccardi, G., Mikušová, K. & Johnsson, K. (2012). *J. Am. Chem. Soc.* **134**, 912–915.
- Wang, W., Zhang, M., Zhang, S., Xu, Z., Li, H., Yu, X. & Wang, W. (2011). *Synlett*, **2011**, 473–476.
- Welch, D. E., Baron, R. R. & Burton, B. A. (1969). *J. Med. Chem.* **12**, 299–303.
- WHO (2018). Global Tuberculosis Report 2018. https://www.who.int/tb/publications/global_report/en/.
- Xu, C., Zhang, L. & Luo, S. (2015). *Org. Lett.* **17**, 4392–4395.
- Zhang, G., Howe, M. & Aldrich, C. C. (2019). *ACS Med. Chem. Lett.* **10**, 348–351.

supporting information

Acta Cryst. (2019). C75, 1031-1035 [https://doi.org/10.1107/S2053229619009185]

Macozinone: revised synthesis and crystal structure of a promising new drug for treating drug-sensitive and drug-resistant tuberculosis

Gang Zhang and Courtney C. Aldrich

Computing details

Data collection: *APEX2* (Bruker, 2013); cell refinement: *SAINT* (Bruker, 2013); data reduction: *SAINT* (Bruker, 2013); program(s) used to solve structure: *SHELXT* (Sheldrick, 2015a); program(s) used to refine structure: *SHELXL2018* (Sheldrick, 2015b); molecular graphics: *OLEX2* (Dolomanov *et al.*, 2009); software used to prepare material for publication: *OLEX2* (Dolomanov *et al.*, 2009).



Crystal data

$C_{20}H_{23}F_3N_4O_3S$
 $M_r = 456.48$
Monoclinic, $P2_1/c$
 $a = 15.051$ (7) Å
 $b = 5.295$ (2) Å
 $c = 26.548$ (11) Å
 $\beta = 97.372$ (7)°
 $V = 2098.3$ (15) Å³
 $Z = 4$

$F(000) = 952$
 $D_x = 1.445 \text{ Mg m}^{-3}$
Mo $K\alpha$ radiation, $\lambda = 0.71073$ Å
Cell parameters from 4036 reflections
 $\theta = 2.7\text{--}27.7^\circ$
 $\mu = 0.21 \text{ mm}^{-1}$
 $T = 205$ K
Block, colourless
0.16 × 0.15 × 0.12 mm

Data collection

Bruker D8 Venture
diffractometer
phi and ω scans
Absorption correction: multi-scan
(SADABS; Bruker, 2014/3)
 $T_{\min} = 0.641$, $T_{\max} = 0.746$
11854 measured reflections

4794 independent reflections
3412 reflections with $I > 2\sigma(I)$
 $R_{\text{int}} = 0.025$
 $\theta_{\max} = 27.7^\circ$, $\theta_{\min} = 1.9^\circ$
 $h = -19 \rightarrow 18$
 $k = -6 \rightarrow 6$
 $l = -26 \rightarrow 34$

Refinement

Refinement on F^2
Least-squares matrix: full
 $R[F^2 > 2\sigma(F^2)] = 0.047$
 $wR(F^2) = 0.122$
 $S = 1.05$
4794 reflections
326 parameters
36 restraints
Primary atom site location: dual

Hydrogen site location: inferred from
neighbouring sites
H-atom parameters constrained
 $w = 1/[\sigma^2(F_o^2) + (0.0422P)^2 + 1.0593P]$
where $P = (F_o^2 + 2F_c^2)/3$
 $(\Delta/\sigma)_{\max} = 0.001$
 $\Delta\rho_{\max} = 0.28 \text{ e \AA}^{-3}$
 $\Delta\rho_{\min} = -0.21 \text{ e \AA}^{-3}$

Special details

Geometry. All esds (except the esd in the dihedral angle between two l.s. planes) are estimated using the full covariance matrix. The cell esds are taken into account individually in the estimation of esds in distances, angles and torsion angles; correlations between esds in cell parameters are only used when they are defined by crystal symmetry. An approximate (isotropic) treatment of cell esds is used for estimating esds involving l.s. planes.

Refinement. Single-crystal X-ray diffraction measurements were carried out on a Bruker SMART APEXII CCD diffractometer at 205.0 K using graphite-monochromated Mo $K\alpha$ radiation ($\lambda = 0.71070 \text{ \AA}$). Absorption correction was performed with Multi-scan BRUKER SADABS. All structures were solved by direct methods and refined by full-matrix least squares on F^2 using the OLEX 2-1.2 computer program package.

Fractional atomic coordinates and isotropic or equivalent isotropic displacement parameters (\AA^2)

	<i>x</i>	<i>y</i>	<i>z</i>	$U_{\text{iso}}^*/U_{\text{eq}}$	Occ. (<1)
S1	0.52703 (3)	0.65072 (11)	0.42522 (2)	0.04694 (16)	
F1	0.8552 (9)	-0.1746 (17)	0.4930 (6)	0.108 (3)	0.54 (2)
F1A	0.8725 (9)	-0.143 (3)	0.4794 (5)	0.111 (4)	0.46 (2)
F2	0.9241 (6)	0.170 (3)	0.4874 (6)	0.128 (4)	0.54 (2)
F2A	0.9244 (7)	0.184 (2)	0.5097 (9)	0.125 (5)	0.46 (2)
F3	0.8780 (7)	0.076 (3)	0.5547 (4)	0.102 (3)	0.54 (2)
F3A	0.8502 (11)	-0.052 (4)	0.5517 (5)	0.129 (5)	0.46 (2)
O1	0.63947 (12)	0.0187 (4)	0.34831 (6)	0.0694 (5)	
O2	0.5728 (11)	0.832 (3)	0.5164 (5)	0.070 (4)	0.5
O3	0.6875 (10)	0.755 (3)	0.5709 (6)	0.081 (4)	0.5
N1	0.54185 (11)	0.3384 (4)	0.34317 (6)	0.0487 (4)	
N2	0.63712 (12)	0.7050 (4)	0.53079 (7)	0.0526 (5)	
N3	0.43493 (11)	0.6421 (4)	0.33536 (6)	0.0515 (5)	
N4	0.26569 (10)	0.7797 (3)	0.28300 (6)	0.0434 (4)	
C1	0.50279 (12)	0.5254 (4)	0.36293 (7)	0.0425 (5)	
C2	0.61018 (13)	0.2030 (5)	0.36797 (7)	0.0464 (5)	
C3	0.65155 (12)	0.2764 (4)	0.42019 (7)	0.0413 (5)	
C4	0.61939 (12)	0.4688 (4)	0.44857 (7)	0.0372 (4)	
C5	0.66502 (12)	0.5100 (4)	0.49754 (7)	0.0410 (5)	
C6	0.73970 (13)	0.3740 (4)	0.51622 (8)	0.0468 (5)	
H6	0.769070	0.407636	0.548954	0.056*	
C7	0.77130 (13)	0.1896 (4)	0.48713 (8)	0.0479 (5)	
C8	0.85604 (17)	0.0546 (6)	0.50615 (10)	0.0662 (7)	
C9	0.72686 (13)	0.1392 (5)	0.43980 (8)	0.0486 (5)	
H9	0.747755	0.009301	0.420233	0.058*	
C10	0.41082 (14)	0.5820 (6)	0.28127 (8)	0.0603 (7)	
H10A	0.439959	0.424089	0.273247	0.072*	
H10B	0.431976	0.716647	0.260462	0.072*	
C11	0.31140 (14)	0.5553 (5)	0.26915 (7)	0.0493 (5)	
H11A	0.296009	0.523696	0.232706	0.059*	
H11B	0.291271	0.409934	0.287546	0.059*	
C12	0.28611 (15)	0.8181 (5)	0.33727 (7)	0.0543 (6)	
H12A	0.266122	0.671138	0.355248	0.065*	
H12B	0.253750	0.966621	0.347326	0.065*	
C13	0.38519 (16)	0.8555 (5)	0.35200 (9)	0.0615 (7)	

H13A	0.404235	1.010959	0.336436	0.074*	
H13B	0.398081	0.873235	0.388956	0.074*	
C14	0.16929 (13)	0.7631 (5)	0.26748 (8)	0.0508 (5)	
H14A	0.139390	0.893787	0.285327	0.061*	
H14B	0.148037	0.598650	0.277928	0.061*	
C15	0.14244 (13)	0.7943 (4)	0.21079 (7)	0.0431 (5)	
H15	0.174017	0.663337	0.193265	0.052*	
C16	0.16959 (17)	1.0481 (5)	0.19249 (9)	0.0625 (6)	
H16A	0.235041	1.062146	0.198156	0.075*	
H16B	0.144881	1.180598	0.212410	0.075*	
C17	0.1376 (2)	1.0897 (6)	0.13692 (10)	0.0831 (9)	
H17A	0.152016	1.262774	0.127726	0.100*	
H17B	0.169625	0.974292	0.116704	0.100*	
C18	0.0386 (2)	1.0477 (6)	0.12409 (11)	0.0823 (9)	
H18A	0.006208	1.179663	0.140110	0.099*	
H18B	0.022299	1.060636	0.087238	0.099*	
C19	0.01126 (18)	0.7948 (6)	0.14168 (10)	0.0745 (8)	
H19A	0.036229	0.662908	0.121730	0.089*	
H19B	-0.054178	0.780856	0.135811	0.089*	
C20	0.04285 (15)	0.7530 (6)	0.19717 (9)	0.0645 (7)	
H20A	0.028111	0.580029	0.206253	0.077*	
H20B	0.010587	0.868432	0.217269	0.077*	
O3A	0.6660 (9)	0.690 (3)	0.5751 (5)	0.063 (2)	0.5
O2A	0.5785 (13)	0.850 (4)	0.5140 (6)	0.080 (4)	0.5

Atomic displacement parameters (\AA^2)

	U^{11}	U^{22}	U^{33}	U^{12}	U^{13}	U^{23}
S1	0.0422 (3)	0.0577 (4)	0.0374 (3)	0.0079 (2)	-0.00828 (19)	-0.0052 (2)
F1	0.092 (5)	0.053 (3)	0.168 (8)	0.019 (3)	-0.029 (5)	-0.001 (3)
F1A	0.079 (5)	0.132 (8)	0.107 (5)	0.066 (5)	-0.043 (4)	-0.058 (6)
F2	0.040 (3)	0.164 (8)	0.183 (8)	0.031 (3)	0.020 (4)	0.080 (6)
F2A	0.048 (4)	0.091 (5)	0.221 (12)	0.001 (3)	-0.047 (6)	-0.023 (7)
F3	0.090 (4)	0.129 (7)	0.074 (3)	0.048 (4)	-0.042 (3)	-0.010 (4)
F3A	0.124 (7)	0.174 (11)	0.085 (5)	0.080 (7)	-0.001 (5)	0.042 (6)
O1	0.0746 (11)	0.0853 (13)	0.0458 (9)	0.0258 (10)	-0.0022 (8)	-0.0171 (9)
O2	0.072 (6)	0.100 (10)	0.035 (4)	0.050 (6)	-0.008 (4)	-0.016 (4)
O3	0.073 (7)	0.091 (9)	0.070 (6)	0.017 (5)	-0.031 (5)	-0.043 (5)
N1	0.0419 (9)	0.0666 (13)	0.0354 (8)	0.0050 (9)	-0.0031 (7)	-0.0064 (9)
N2	0.0508 (10)	0.0619 (13)	0.0419 (10)	0.0087 (10)	-0.0067 (8)	-0.0093 (9)
N3	0.0428 (9)	0.0688 (13)	0.0390 (9)	0.0082 (9)	-0.0094 (7)	-0.0053 (9)
N4	0.0404 (9)	0.0533 (11)	0.0337 (8)	0.0026 (8)	-0.0065 (6)	-0.0019 (8)
C1	0.0327 (9)	0.0573 (14)	0.0354 (9)	-0.0037 (9)	-0.0033 (7)	0.0010 (9)
C2	0.0411 (10)	0.0625 (15)	0.0353 (10)	0.0037 (10)	0.0037 (8)	-0.0052 (10)
C3	0.0338 (9)	0.0532 (13)	0.0362 (10)	-0.0008 (9)	0.0014 (7)	0.0007 (9)
C4	0.0305 (9)	0.0463 (12)	0.0337 (9)	-0.0029 (8)	-0.0002 (7)	0.0025 (8)
C5	0.0369 (10)	0.0489 (13)	0.0357 (10)	-0.0004 (9)	-0.0018 (7)	-0.0031 (9)
C6	0.0384 (10)	0.0585 (14)	0.0405 (10)	-0.0007 (10)	-0.0066 (8)	-0.0007 (10)

C7	0.0365 (10)	0.0575 (14)	0.0474 (11)	0.0065 (10)	-0.0032 (8)	0.0002 (11)
C8	0.0518 (14)	0.0741 (19)	0.0668 (16)	0.0172 (13)	-0.0144 (12)	-0.0065 (14)
C9	0.0382 (10)	0.0606 (15)	0.0463 (11)	0.0061 (10)	0.0029 (8)	-0.0055 (11)
C10	0.0479 (12)	0.098 (2)	0.0328 (10)	0.0152 (13)	-0.0042 (9)	-0.0019 (12)
C11	0.0487 (11)	0.0646 (15)	0.0319 (10)	0.0043 (11)	-0.0056 (8)	-0.0067 (10)
C12	0.0557 (12)	0.0663 (16)	0.0369 (10)	0.0179 (11)	-0.0095 (9)	-0.0117 (10)
C13	0.0616 (14)	0.0593 (15)	0.0552 (13)	0.0123 (12)	-0.0248 (11)	-0.0148 (12)
C14	0.0394 (10)	0.0706 (16)	0.0403 (11)	0.0025 (10)	-0.0025 (8)	0.0004 (10)
C15	0.0428 (10)	0.0447 (12)	0.0386 (10)	0.0037 (9)	-0.0070 (8)	-0.0023 (9)
C16	0.0654 (15)	0.0550 (15)	0.0618 (14)	-0.0078 (12)	-0.0122 (11)	0.0056 (12)
C17	0.098 (2)	0.081 (2)	0.0654 (17)	-0.0008 (17)	-0.0073 (15)	0.0278 (16)
C18	0.100 (2)	0.0721 (19)	0.0639 (16)	0.0223 (17)	-0.0313 (15)	0.0081 (15)
C19	0.0699 (16)	0.078 (2)	0.0659 (16)	0.0025 (14)	-0.0305 (13)	-0.0043 (14)
C20	0.0483 (12)	0.0796 (18)	0.0602 (14)	-0.0067 (13)	-0.0136 (10)	0.0029 (13)
O3A	0.062 (5)	0.082 (7)	0.039 (2)	0.011 (4)	-0.018 (3)	-0.016 (3)
O2A	0.090 (8)	0.060 (6)	0.080 (8)	0.026 (5)	-0.027 (6)	-0.020 (5)

Geometric parameters (\AA , $^{\circ}$)

S1—C1	1.776 (2)	C9—H9	0.9400
S1—C4	1.739 (2)	C10—H10A	0.9800
F1—C8	1.262 (10)	C10—H10B	0.9800
F1A—C8	1.305 (11)	C10—C11	1.496 (3)
F2—C8	1.342 (9)	C11—H11A	0.9800
F2A—C8	1.229 (11)	C11—H11B	0.9800
F3—C8	1.293 (9)	C12—H12A	0.9800
F3A—C8	1.347 (10)	C12—H12B	0.9800
O1—C2	1.216 (3)	C12—C13	1.506 (3)
O2—N2	1.200 (16)	C13—H13A	0.9800
O3—N2	1.253 (14)	C13—H13B	0.9800
N1—C1	1.296 (3)	C14—H14A	0.9800
N1—C2	1.353 (3)	C14—H14B	0.9800
N2—C5	1.455 (3)	C14—C15	1.516 (3)
N2—O3A	1.203 (14)	C15—H15	0.9900
N2—O2A	1.211 (18)	C15—C16	1.504 (3)
N3—C1	1.330 (2)	C15—C20	1.512 (3)
N3—C10	1.470 (3)	C16—H16A	0.9800
N3—C13	1.455 (3)	C16—H16B	0.9800
N4—C11	1.444 (3)	C16—C17	1.508 (3)
N4—C12	1.449 (2)	C17—H17A	0.9800
N4—C14	1.459 (2)	C17—H17B	0.9800
C2—C3	1.496 (3)	C17—C18	1.501 (4)
C3—C4	1.390 (3)	C18—H18A	0.9800
C3—C9	1.390 (3)	C18—H18B	0.9800
C4—C5	1.407 (3)	C18—C19	1.494 (4)
C5—C6	1.373 (3)	C19—H19A	0.9800
C6—H6	0.9400	C19—H19B	0.9800
C6—C7	1.368 (3)	C19—C20	1.505 (3)

C7—C8	1.492 (3)	C20—H20A	0.9800
C7—C9	1.372 (3)	C20—H20B	0.9800
C4—S1—C1	100.61 (10)	N4—C11—H11B	109.4
C1—N1—C2	124.30 (17)	C10—C11—H11A	109.4
O2—N2—O3	121.8 (11)	C10—C11—H11B	109.4
O2—N2—C5	119.3 (6)	H11A—C11—H11B	108.0
O3—N2—C5	118.3 (9)	N4—C12—H12A	109.5
O3A—N2—C5	116.8 (9)	N4—C12—H12B	109.5
O3A—N2—O2A	123.7 (11)	N4—C12—C13	110.69 (18)
O2A—N2—C5	118.8 (7)	H12A—C12—H12B	108.1
C1—N3—C10	120.85 (19)	C13—C12—H12A	109.5
C1—N3—C13	125.62 (17)	C13—C12—H12B	109.5
C13—N3—C10	113.11 (17)	N3—C13—C12	110.48 (19)
C11—N4—C12	108.74 (16)	N3—C13—H13A	109.6
C11—N4—C14	111.55 (17)	N3—C13—H13B	109.6
C12—N4—C14	111.45 (16)	C12—C13—H13A	109.6
N1—C1—S1	127.78 (15)	C12—C13—H13B	109.6
N1—C1—N3	119.23 (18)	H13A—C13—H13B	108.1
N3—C1—S1	112.98 (16)	N4—C14—H14A	108.8
O1—C2—N1	120.73 (19)	N4—C14—H14B	108.8
O1—C2—C3	118.38 (19)	N4—C14—C15	113.72 (17)
N1—C2—C3	120.89 (19)	H14A—C14—H14B	107.7
C4—C3—C2	124.04 (17)	C15—C14—H14A	108.8
C9—C3—C2	115.71 (19)	C15—C14—H14B	108.8
C9—C3—C4	120.25 (18)	C14—C15—H15	107.9
C3—C4—S1	122.06 (14)	C16—C15—C14	111.66 (18)
C3—C4—C5	116.85 (17)	C16—C15—H15	107.9
C5—C4—S1	121.09 (16)	C16—C15—C20	110.74 (19)
C4—C5—N2	121.74 (18)	C20—C15—C14	110.58 (18)
C6—C5—N2	116.08 (17)	C20—C15—H15	107.9
C6—C5—C4	122.16 (19)	C15—C16—H16A	109.1
C5—C6—H6	120.1	C15—C16—H16B	109.1
C7—C6—C5	119.89 (18)	C15—C16—C17	112.4 (2)
C7—C6—H6	120.1	H16A—C16—H16B	107.9
C6—C7—C8	119.7 (2)	C17—C16—H16A	109.1
C6—C7—C9	119.47 (19)	C17—C16—H16B	109.1
C9—C7—C8	120.8 (2)	C16—C17—H17A	109.1
F1—C8—F2	108.5 (8)	C16—C17—H17B	109.1
F1—C8—F3	110.5 (7)	H17A—C17—H17B	107.8
F1—C8—C7	112.9 (6)	C18—C17—C16	112.6 (2)
F1A—C8—F3A	101.1 (8)	C18—C17—H17A	109.1
F1A—C8—C7	114.4 (5)	C18—C17—H17B	109.1
F2—C8—C7	108.4 (5)	C17—C18—H18A	109.3
F2A—C8—F1A	105.8 (9)	C17—C18—H18B	109.3
F2A—C8—F3A	108.2 (7)	H18A—C18—H18B	108.0
F2A—C8—C7	115.5 (7)	C19—C18—C17	111.5 (2)
F3—C8—F2	102.6 (5)	C19—C18—H18A	109.3

F3—C8—C7	113.2 (4)	C19—C18—H18B	109.3
F3A—C8—C7	110.6 (5)	C18—C19—H19A	109.2
C3—C9—H9	119.3	C18—C19—H19B	109.2
C7—C9—C3	121.3 (2)	C18—C19—C20	111.9 (2)
C7—C9—H9	119.3	H19A—C19—H19B	107.9
N3—C10—H10A	109.6	C20—C19—H19A	109.2
N3—C10—H10B	109.6	C20—C19—H19B	109.2
N3—C10—C11	110.19 (17)	C15—C20—H20A	109.0
H10A—C10—H10B	108.1	C15—C20—H20B	109.0
C11—C10—H10A	109.6	C19—C20—C15	113.1 (2)
C11—C10—H10B	109.6	C19—C20—H20A	109.0
N4—C11—C10	111.31 (19)	C19—C20—H20B	109.0
N4—C11—H11A	109.4	H20A—C20—H20B	107.8
S1—C4—C5—N2	0.2 (3)	C6—C7—C8—F2A	-67.1 (12)
S1—C4—C5—C6	-177.98 (16)	C6—C7—C8—F3	18.7 (9)
O1—C2—C3—C4	-174.1 (2)	C6—C7—C8—F3A	56.3 (13)
O1—C2—C3—C9	6.2 (3)	C6—C7—C9—C3	1.7 (3)
O2—N2—C5—C4	1.0 (11)	C8—C7—C9—C3	-175.3 (2)
O2—N2—C5—C6	179.3 (11)	C9—C3—C4—S1	178.49 (16)
O3—N2—C5—C4	-170.4 (7)	C9—C3—C4—C5	-1.7 (3)
O3—N2—C5—C6	7.9 (8)	C9—C7—C8—F1	-37.8 (9)
N1—C2—C3—C4	5.9 (3)	C9—C7—C8—F1A	-13.4 (11)
N1—C2—C3—C9	-173.8 (2)	C9—C7—C8—F2	82.5 (9)
N2—C5—C6—C7	-179.0 (2)	C9—C7—C8—F2A	109.9 (12)
N3—C10—C11—N4	56.2 (3)	C9—C7—C8—F3	-164.3 (8)
N4—C12—C13—N3	-56.6 (3)	C9—C7—C8—F3A	-126.7 (13)
N4—C14—C15—C16	-61.0 (3)	C10—N3—C1—S1	173.83 (17)
N4—C14—C15—C20	175.2 (2)	C10—N3—C1—N1	-7.3 (3)
C1—S1—C4—C3	-2.88 (19)	C10—N3—C13—C12	51.9 (3)
C1—S1—C4—C5	177.31 (17)	C11—N4—C12—C13	61.2 (2)
C1—N1—C2—O1	174.7 (2)	C11—N4—C14—C15	-73.9 (2)
C1—N1—C2—C3	-5.3 (3)	C12—N4—C11—C10	-61.4 (2)
C1—N3—C10—C11	135.4 (2)	C12—N4—C14—C15	164.3 (2)
C1—N3—C13—C12	-135.5 (2)	C13—N3—C1—S1	1.8 (3)
C2—N1—C1—S1	0.1 (3)	C13—N3—C1—N1	-179.3 (2)
C2—N1—C1—N3	-178.6 (2)	C13—N3—C10—C11	-51.6 (3)
C2—C3—C4—S1	-1.2 (3)	C14—N4—C11—C10	175.31 (17)
C2—C3—C4—C5	178.66 (19)	C14—N4—C12—C13	-175.5 (2)
C2—C3—C9—C7	179.5 (2)	C14—C15—C16—C17	-175.9 (2)
C3—C4—C5—N2	-179.62 (18)	C14—C15—C20—C19	177.0 (2)
C3—C4—C5—C6	2.2 (3)	C15—C16—C17—C18	53.5 (3)
C4—S1—C1—N1	3.8 (2)	C16—C15—C20—C19	52.7 (3)
C4—S1—C1—N3	-177.46 (16)	C16—C17—C18—C19	-53.5 (4)
C4—C3—C9—C7	-0.2 (3)	C17—C18—C19—C20	53.2 (3)
C4—C5—C6—C7	-0.8 (3)	C18—C19—C20—C15	-53.7 (3)
C5—C6—C7—C8	175.8 (2)	C20—C15—C16—C17	-52.2 (3)
C5—C6—C7—C9	-1.2 (3)	O3A—N2—C5—C4	163.6 (6)

C6—C7—C8—F1	145.3 (9)	O3A—N2—C5—C6	−18.1 (7)
C6—C7—C8—F1A	169.7 (10)	O2A—N2—C5—C4	−7.0 (11)
C6—C7—C8—F2	−94.5 (8)	O2A—N2—C5—C6	171.2 (11)

Hydrogen-bond geometry (Å, °)

D—H···A	D—H	H···A	D···A	D—H···A
N2—O2···H12 <i>B</i>	0.98 (1)	2.68 (1)	3.311 (3)	123 (1)
N2—O3···H13 <i>B</i>	0.98 (1)	2.94 (1)	3.844 (15)	153 (1)